

Long-term Detailed Monitoring and Energy Performance Evaluation of a Ground Source Heat Pump System. A Study Case in Catalonia

Jordi García-Céspedes¹, Ignasi Herms², Georgina Arnó², José Juan de Felipe³

¹ Energía Coherente, C/ Nord 2 Bj.C, E-08004 Barcelona;

² Institut Cartogràfic i Geològic de Catalunya (ICGC), Parc Montjuïc E-08038, Barcelona, Spain;

³ Department of Mining, Industrial and ICT Engineering. Universitat Politècnica de Catalunya (UPC), Av/ Bases de Manresa 61, E-08242 Manresa. Barcelona. Spain

jordi.garcia@energiacoherente.com; ignasi.herms@icgc.cat; georgina.arno@icgc.cat; jose.juan.de.felipe@upc.edu

Keywords: Ground source heat pump, Seasonal performance, Monitoring system, data-driven diagnostics, data-driven fault detection

ABSTRACT

An exhaustive data analysis was undertaken in a remotely monitored shallow geothermal energy (SGE) installation. The system operates since 2012 as the heating and cooling facility of an office building located in Tremp (Lleida, Spain). The performance parameters recorded by its monitoring system account basically for the flow rates and flow temperatures, heating, domestic hot water production and cooling, electrical energy consumption and compressor operation time of the ground source heat pump (GSHP). Through the proper selection of the sampling frequency (minute-resolved) and a smart data processing, it was demonstrated the potential of continuous monitoring plus data analysis as an effective and efficient tool for diagnostics and fault-detection in GSHPs operating under real conditions. In particular, a faulty 3-way valve was identified thanks to the analysis of the data, and a progressive degradation in performance was identified and quantified. This fact motivated extra physical inspection that brought up new maintenance needs. The results of the analysis were supported by simulations carried out under Ground Loop Design software environment, and several sensitivity analyses were carried out to evaluate the influence of key parameters of the installation on its seasonal performance. As a result, this work opened new opportunities for the optimization of GSHP seasonal performance.

1. INTRODUCTION

A “suspicious” low performance in a shallow geothermal energy (SGE) installation can have several origins. It can be due to a faulty device, a deficient maintenance, or in the worst case scenario, due to a bad design of the whole installation. In the latter case, little can be done apart from learning for the next project. But in the first two cases, as much information as possible must be gathered in order to detect, identify or quantify any possible fault, performance degradation or room for optimisation. However, many installations are commissioned and maintained by different entities, and this fact usually brings along certain loss of information from the installers to the maintainers and finally to the final users. Additionally, it is a common practice that operation and maintenance actions stay limited to switching between operation modes every change of season, checking the alarms installed in the system (and reacting accordingly), etc. Although this can be understood in residential, small-size installations (usually no higher than 10 kW), medium (≥ 25 kW) and large (≥ 100 kW) SGE installations deserve an extra investment in a more proactive management. The usual warnings that an alarms panel can provide are devoted to inform about the total or partial shut-down of the unit in order to avoid its breakdown. But there is no alarm capable of warning the user about a progressive degradation of the performance (although this could be indicating an upcoming failure mechanism), and of course there is no alarm capable of telling us how far we are from optimal performance. In this case, a detailed and reliable monitoring system is essential, but it is even more essential to analyse the data acquired and recorded by it in order to reduce the “performance gap” [Spitler and Gehlin, 2019].

Nomenclature

COP	Coefficient of performance [-]	Subscripts	
EER	Energy Efficiency ratio [-]	ON	Compressor(s) ON
SCOP	Seasonal <i>COP</i> [-]	OFF	Compressor(s) OFF
SEER	Seasonal <i>EER</i> [-]	brine	Concerning heat exchanger liquid (ground source)
PLF	Part-Load Factor [-]	h	Concerning heat production
PLR	Part-Load Ratio [-]	c	Concerning heat rejection (cooling)
DHW	Domestic Hot Water	e	Concerning electric energy consumption
SV	Storage Vessel	pump	Concerning circulation pump(s)
E	Energy [kWh]	Superscripts	
t	Time [min]	in	At the entrance
P	Power (kW)	out	At the exit
		A	Concerning heat pump module / compressor A
		B	Concerning heat pump module / compressor B

The aim of this work is to demonstrate how data-driven diagnostics and simulation tools can provide relevant and useful information about the performance of SGE installations, from a practical perspective and presenting a set of particular fault events detected and characterised on a case study. The details of the data-processing methodology and metrics employed, as well as a detailed description of the case study have been already described in [García-Céspedes et al. 2019a] and [García-Céspedes et al. 2019b]. Here only the most relevant aspects of the case study related to the present work will be presented. Finally, this analysis is limited to the production stage of the building, leaving the distribution stage for further analysis.

2. CASE STUDY. DESCRIPTION

The SGE installation under study (see Figure 1) is located in Tremp (Catalonia, Spain). It provides heating, cooling and DHW to a medium-size office building thanks a vertical closed-loop borehole heat exchanger (BHE) field in combination with a ground source heat pump (GSHP). The BHE field consists of 10 boreholes with an average depth of 140 m each (1400 m in total), separated between 5 and 6 m from each other, forming a linear array with a 90 ° bent in the middle. The nominal capacity installed is 60 kW, that is provided by a brine-to-water heat pump from the Swedish company Nibe Industrier AB (model Fighter 1330-60). The heat pump consists of two twin fixed-speed compressors (modules A and B) operating in parallel. Module A acts as the master, while module B acts as the slave. Besides, DHW is produced exclusively by module B. The SGE installation shifts from heating to cooling mode thanks to a climate exchanger module (CEM) that contains a set of four different 3-way valves to divert the brine (pure water in this case) from the ground towards the evaporator stage (cool season) or the condenser stage (warm season). A storage vessel (SV) accumulates cold and hot water (warm and cool seasons, respectively) and acts as a thermal buffer tank between the GSHP and the building distribution circuit in order to avoid excessive start-stop cycling of the compressors. Another tank is used to accumulate hot water for DHW production (DHW vessel), with the same objective as the SV. Although the heat pump is equipped with a smart algorithm to decide automatically the heating or cooling set point according to the ambient temperature (heating curves), the set temperatures of the SV and DHW vessel ($T_{SV}^{setpoint}$ and $T_{DHW}^{setpoint}$, respectively) are forced to be constant along the year regardless of the ambient conditions. These values are 10 and 42 °C for the SV (warm and cool seasons, respectively) and 38 °C for the DHW vessel. The time between successive heating/cooling cycles is not determined by a classical deadband. Instead, the heat pump waits until the next ON period based on a constant factor expressed in “degree-minutes”. This factor is 400 °C·min under heating mode, and 200 °C·min under cooling mode. Notice that the primary circuit (ground side) and the secondary circuit (building) are not isolated and share the same heat exchanging fluid (water), except for the DHW, which flows through an independent pipe circuit for hygiene reasons. The circulation of the fluid at the evaporator side is carried out by an external pump, while two smaller internal pumps are used at the condenser side. The external pump operates whenever the heat pump is ON, while each of the internal pumps activates only if the corresponding module (A or B) are ON. Moreover, the system performance is monitored through a set of temperature sensors and energy meters. The readouts of these sensors and meters are collected by a data acquisition unit and displayed on a web portal. The main parameters accessible and periodically recorded by the monitoring system are E_h , E_c , E_{DHW} , E_e , T_{SV}^{out} , T_{brine}^{out} , T_{brine}^{in} , t_{ON}^A and t_{ON}^B . The time resolution varies from weekly-averaged (WA), to 30-minute-averaged (30MA) and minute-resolved (MR) values.

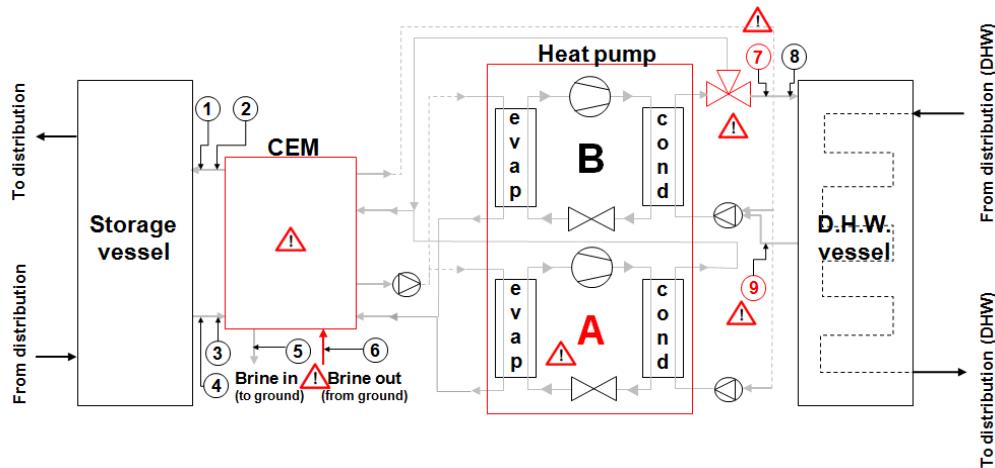


Figure 1. Basic scheme of the heating/cooling production facility under study (extracted and modified from [García-Céspedes et al., 2019a]): 1.-Upper temperature sensor; 2.-Volumetric flow sensor; 3.- Lower temperature sensor (these 3 sensors account for thermal energy measurement at the SV); 4.- SV temperature sensor; 5.- Temperature sensor for brine (water) going to the ground; 6.- Temperature sensor for brine (water) coming from the ground; 7.- Upper temperature sensor; 8.- Volumetric flow sensor; 9.- Lower temperature sensor (these 3 sensors account for thermal energy measurement at the DHW vessel). The elements that were identified as degraded or malfunctioning are marked in red.

The different modes of operation of the SGE installation are illustrated by Figure 2. Basically, the heat can flow in four different manners thanks to the CEM and an additional 3-way valve at the exit of the module B (condenser outlet):

- Heating mode (red arrows): The heat is extracted from the ground and injected into the SV or the DHW vessel. To divert the heat flow to one tank or the other depends on the position of the 3-way valve at the exit of the condenser in module B. It is not possible to produce DHW with module A.

- Cooling mode (blue arrows): The heat can be extracted from the building and injected into the ground or use it as a heat source for DHW production. The latter configuration allows the system to achieve high COP values (over 5), since useful heating and cooling are produced simultaneously in the same run. However, this operating mode is residual compared with regular heating or cooling, so its contribution to seasonal performance is not really relevant.
- DHW production during warm season (orange arrows): The heat is extracted from the ground and injected into the DHW vessel, analogously as in the case of heat production during the warm season.

Thanks to data analysis, several faulty devices along with a degraded performance of the heat pump were detected (marked in red on Figure 1). This process also yielded a reliable model of the SGE installation [García-Céspedes et al., 2019a] within the case study. The software used was Ground Loop Design (GLD) environment [Thermal dynamics Inc. version 2016], which enabled the simulation of different system variations (sensitivity analysis). This contributed to plan future optimisation strategies. In the following sections the results of the analysis will be presented and discussed.

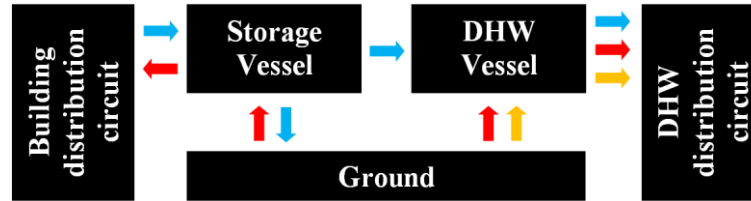


Figure 2: Diagram illustrating the different operation modes of the SGE installation. Heat flow during the cool season is depicted by red arrows. Blue and orange arrows show the different paths of heat flow during the warm season.

3. RESULTS

A thorough analysis of the SGE installation described above provided a remarkable amount of relevant information about its operation and performance. In contrast, it is hard to imagine that this information could be generated by the established maintenance routine. Here are described two data-driven fault detections and the identification and characterisation of two origins of performance degradation. When the data analysis started out in January 2017, the first step was to check the availability of data recorded by the monitoring system, and the first anomalous observation was related to the DHW production. By looking at the weekly-accumulated values of E_{DHW} , it was identified (apparently) DHW production only during the warm season, which was intrinsically suspicious, because a higher DHW demand should be expected during the cool season. After checking that DHW was effectively being consumed at the building during the cool season, a deeper look was carried out, looking at the MR data. In Figure 3 it is shown a plot of E_c , E_{DHW} , E_e , T_{brine}^{out} , T_{brine}^{in} , T_{SV}^{out} , along with the compressor operation times t_{ON}^A and t_{ON}^B . The sampling period lasts for 60 minutes in two separates dates: before and after the problems identified were solved. In the left plots (18th of May of 2017), three periods are clearly differentiated. The first one corresponds to a simple cooling period, where the heat from the building is extracted towards the ground using the master compressor A. This translates as a decreasing T_{SV}^{out} . In the second period, the cooling demand of the building grows, so the slave compressor B switches ON to aid the compressor A. T_{SV}^{out} decreases at a faster rate, while the difference between T_{brine}^{out} and T_{brine}^{in} gets more pronounced. In the third period, the compressor A switches OFF and only compressor B stays operative. This scenario corresponds, by definition, to the production of DHW using the heat rejected from the building as the heat source. However, only 1kWh of DHW production is recorded by the monitoring system, while 7 kWh of heat rejection is observed. Besides, another strange event takes place simultaneously: although T_{brine}^{in} approaches to T_{brine}^{out} during the first minutes of the 3rd period (as expected), after a few minutes it suffers an anomalous rise over 35 °C. This is truly anomalous, because even under the most demanding scenario for cooling mode (compressors A and B operative), T_{brine}^{in} was under 30°C just a few minutes ago. Additionally, since the heat is extracted from the building and not from the ground, it is absurd to observe any affection to T_{brine}^{in} due to this operation mode. Therefore, two different problems were identified at this time. On the one hand, while a non-zero amount of E_{DHW} was being recorded throughout the warm season, it was demonstrated that it did not correspond to the precise moments when only compressor B was operative. On the other hand, an anomalous rise in T_{brine}^{in} was observed during the periods when only compressor B was ON in combination with cooling production. These observations triggered a physical inspection in the installation which led to the identification of the causes behind both problems. Actually the two problems were linked. It was found that the temperature sensors T_{DHW}^{in} and T_{DHW}^{out} (represented by numbers 7 and 9 in Figure 1) were exchanged at the entrance of the energy meter (number 8 in Figure 1) probably by mistake during the installation. Therefore, the natural cool-down process of the DHW vessel was interpreted by the energy meter as heat production.

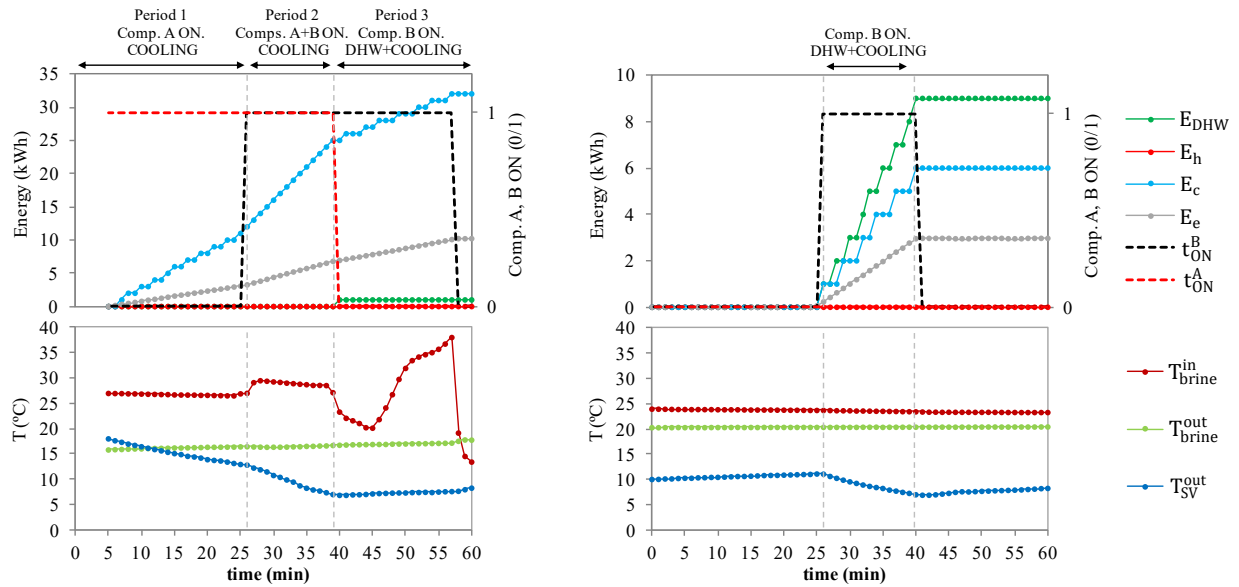


Figure 3: Energy and temperature recordings during 1h, the 18th of May 2017 (left) and the 3rd of September 2018 (right).

Nevertheless, in order to measure a heat flow it was necessary an actual liquid flow entering and exiting the DHW vessel, and in fact this is what was happening. Thanks to these observations, it was demonstrated that the 3-way valve located at the exit of the condenser stage in module B was failing to divert the brine from the condenser towards the DHW vessel or towards the ground. If the position of the 3-way valve outlet is not completely set to one way or the other, the brine flow coming from the condenser will split into two: one part will go to the DHW vessel, but the other will go to the ground. This explained finally why $T_{\text{brine}}^{\text{in}}$ rose so much. In addition, the delay observed until the anomalous rise of $T_{\text{brine}}^{\text{in}}$ was attributed to the fact that the “leaking” brine was pushed against a circuit with higher pressure drop than that going to the DHW vessel. In the right plots of Figure 3 (3rd of September of 2018), the $T_{\text{DHW}}^{\text{in}}$ and $T_{\text{DHW}}^{\text{out}}$ sensors were already in place (since the 28th of July of 2017), and the 3-way valve had been already replaced (since the 23rd of December of 2017). For this reason the recording of E_{DHW} coincides with the actual measuring of DHW production, and $T_{\text{brine}}^{\text{in}}$ stays unaffected throughout the observed period.

By looking at the big picture, it was possible to identify a progressive degradation in performance of the whole system. In Figure 4, WA data corresponding to the COP (left) and EER (right) along 4 complete seasons show clearly how the system performance is decreasing with time beyond the natural drop occurring within each seasonal period. This observation was more pronounced in the case of the EER. The linear approximation of the yearly average decreasing rate was 2.0% for the COP and 3.8% for the EER, considering the first 3 seasons in each case. This result was already presented in [García-Céspedes et al. 2019a], but then it was mentioned a physical inspection carried out at the beginning of August of 2018. During this physical inspection, it was found a faulty 3-way valve within the CEM, causing an unwanted connection between the primary and secondary circuits. In addition, the water filter of the evaporator was cleaned up. Since then, enough data has been collected again in order to see the effects (or not) of such intervention. The dashed line on each of the plots in Figure 4 represents a new linear approximation of the performance decreasing rate, including a new season. In both cases, the slope of the linear approximation diminishes, which reveals a slight improvement in the decreasing performance trend. Nonetheless, the trend continues towards lower values of COP and EER year after year.

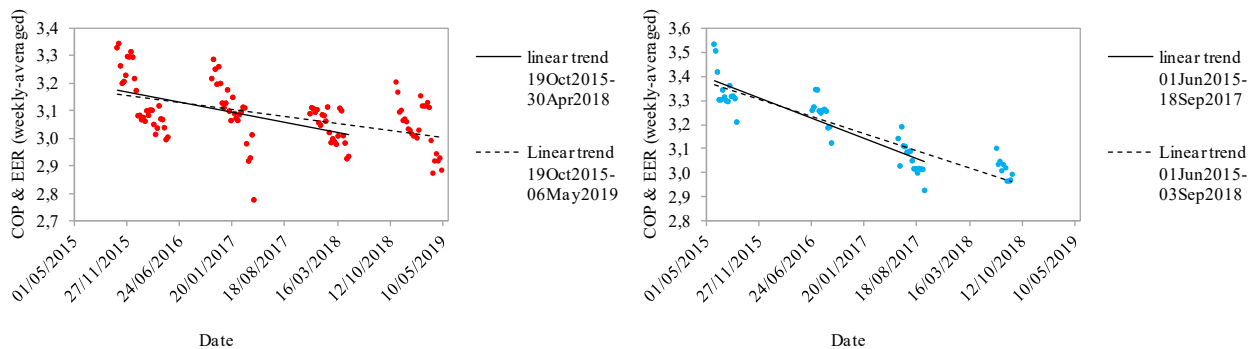


Figure 4: WA-COP (left) and WA-EER (right) evolution through time. Linear trend is evaluated for the first 3 seasons and for all of them.

When going into detail in the analysis of the GSHP performance, additional and relevant information was obtained. In [García-Céspedes et al. 2019a] a new methodology was presented in order to analyse not only the partialisation losses of a GSHP equipped with two parallel compressor stages, but also the difference between declared and actual performance of a GSHP. This methodology was based in the correlation between the part-load factor (PLF) and the part-load ratio (PLR) applied to a GSHP operating under real operation conditions. MR data was required in such analysis. As a result, it was concluded that despite the

presence of a relative large storage vessel (750 l) and the smart configuration of the heat pump (2 parallel modules instead of a single one), the GSHP showed significant losses due to part-load operation, in the order of 8-9% when PRL approaches to 0. Besides, the actual capacity of the GSHP was quantified as 7% and 11% below the declared values by the manufacturer (for the cool and warm seasons, respectively). The origin of such capacity reduction is not yet known. Although these results are within the tolerance margin established by norm EN-14511 (2008), it was surprising the difference in capacity reduction observed depending on the season. This fact led to hypothesise about a more pronounced degradation of module A with respect to module B due to a more intense operation of the first one. Anyhow, the characterisation of the partialisation losses contributed to a consistent and reliable modelling of the system under GLD environment, which yielded a remarkable coincidence between measured and simulated seasonal performance.

4. DISCUSSION

4.1. Causes, consequences and correlations

It is important to discuss the implications of the faulty 3-way valve, from a global perspective, in order to assess its relevance in the measurements carried out until the moment of its replacement. For this it is necessary to distinguish between operating modes:

- During the warm season, under regular cooling mode (with modules A or A+B ON), part of the water flow going from the outlet of the condenser (module B) towards the ground was pushed against the DHW vessel, creating a circulating flow in the DHW vessel, and therefore the outlet flow of the DHW vessel was mixed with the brine flow coming from the ground at the inlet of the condenser. In this case $T_{DHW}^{in} < T_{DHW}^{out}$. Consequently, the water at the DHW vessel would cool down and the energy meter should measure cooling, but due to the exchanged position of the temperature sensors, the energy meter was interpreting it as heating, and this was the heating recorded by monitoring system during the warm season. In parallel, the efficiency of the process would be reduced because of the rise in the temperature at the entrance of the condenser in module B compared to normal operation.
- During the warm season, under special cooling mode (the heat rejected by the building is used to produce DHW), part of the water flow going from the outlet of the condenser towards the DHW vessel was pushed towards the ground, creating a circulating flow in the ground circuit. For this reason an anomalous high temperature was observed in the readout of T_{brine}^{in} . Now $T_{DHW}^{in} > T_{DHW}^{out}$ and the energy meter was supposed to measure heating, but this energy production was interpreted as cooling instead, so the monitoring system did not record it.
- During the cool season, the situation was different, because there was no possible mechanism to measure cooling by the DHW energy meter (and actually, this explains why no E_{DHW} recordings were observed during the cool season). The reason was that under heating mode an unwanted water flow was being pushed to the DHW vessel with a higher temperature than that already contained in it (notice also that $T_{SV}^{setpoint} = 42^\circ\text{C}$ and $T_{DHW}^{setpoint} = 38^\circ\text{C}$ during the cool season). So if there was any leakage of heating fluid during heating, it would actually contribute to produce DHW (that sooner or later would be required) at the cost of a longer time required to reach the set point in the SV.
- During the cool season, when producing DHW, part of the water flow at the outlet of the condenser was pushed towards to the storage vessel. In this case this fact could contribute to heat or cool the water in the SV, depending on the value of T_{SV}^{out} at that moment, but generally it would help to keep it warm. In this particular case, part of the energy devoted to produce DHW would be measured as E_h by the energy-meter of the storage vessel. Anyway, the cost of reaching the set point in the DHW vessel would be a longer required time.

In order to find out or discard correlations between the decreasing performance and other parameters, the evolution of T_{brine}^{out} was evaluated (Figure 5, left). However, no significant trend could be identified within the experimental error, so the decreasing performance factor could not be attributed to any change in the ground dynamics yet. Moreover, it was not possible to establish a relationship between performance and seasonal load. As seen in Figure 5 (right), the cooling and heating demand of the building does not follow a clear trend all over the years.

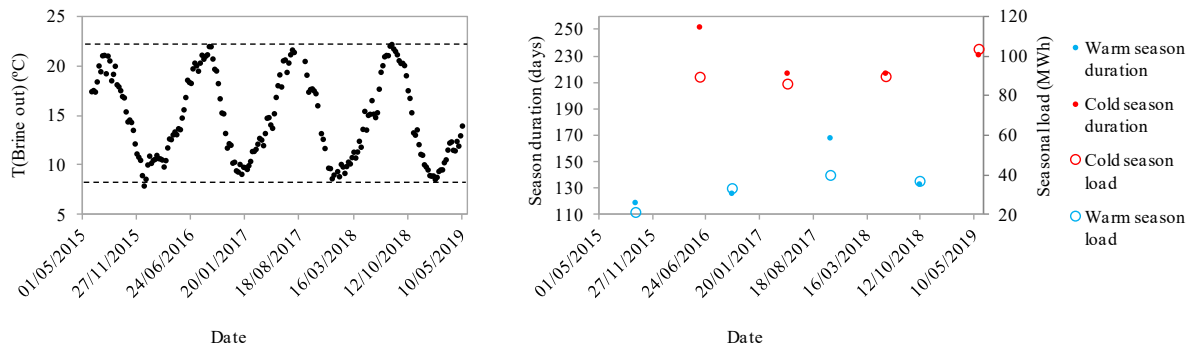


Figure 5: Time evolution of the T_{brine}^{out} (WA values) (left) and seasonal loads and season duration (right).

However, a clear increasing trend of the average day load can be identified (Figure 6). The observed increase in average day load should contribute to a COP/EER improvement, not the opposite, because a higher day load means a higher PRL and therefore lower partialisation losses (higher PLF). On the other hand, an increase of the overall thermal load should contribute to a worse performance in general, but the evolution of the ground temperatures does not corroborate this aspect. Hence the dynamics

associated to the building demand should be discarded as well as a plausible cause behind the progressive descent observed in heating and cooling performance.

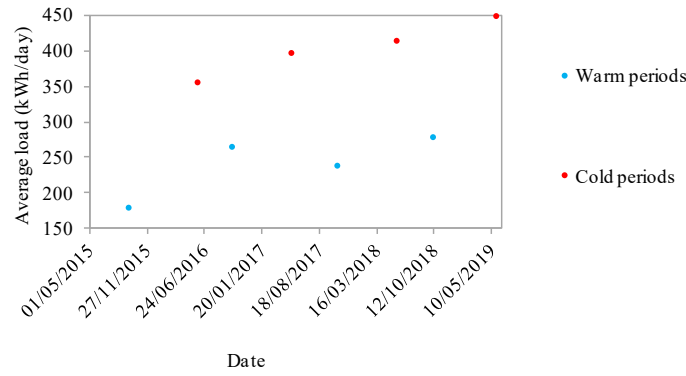


Figure 6: Time evolution of the daily average load, obtained as the ratio between seasonal load and season duration.

4.2. Optimisation strategies

In addition to the data-driven diagnostics, simulation is a revealing (and useful) tool to test different strategies in order to optimise the performance of the SGE installation, in a virtual manner. The modelling of the installation and the reproduction of its actual performance is described in detailed in [García-Céspedes et al., 2019a]. Thanks to this model, it was possible to perform several sensitivity analyses in order to find the most relevant parameters for the performance of the installation, in a quantitative way. Figure 7 shows the influence of $T_{SV}^{setpoint}$ during the warm season (left plot) and during the cool season (right plot). The simulations point to a significant influence of $T_{SV}^{setpoint}$ in order to increase the GSHP seasonal performance factor, especially during the warm season (SEER). In particular, an increase of 3 °C in $T_{SV}^{setpoint}$ would yield a 28 % rise in the SEER. Although the SCOP is not so sensitive to $T_{SV}^{setpoint}$, to reduce its value during the cool season from 42 to 35 °C would improve the SCOP by a 17%. However, to modify the $T_{SV}^{setpoint}$ in such a way has an important counterpart. The higher the difference between room temperature (normally around 21 °C during the cool season, and 24 °C during the warm season) and $T_{SV}^{setpoint}$, the more efficient the heat transfer will be between the building and the SGE installation. So the benefit of reducing this gap is not evident. The key point is that along the season, $T_{SV}^{setpoint}$ can certainly be varied and adapted to the different heat gains and losses of the building. So the best action to take would be to change the settings of the GHSP in order to calculate automatically the optimum value of $T_{SV}^{setpoint}$ depending on the ambient temperature in each moment.

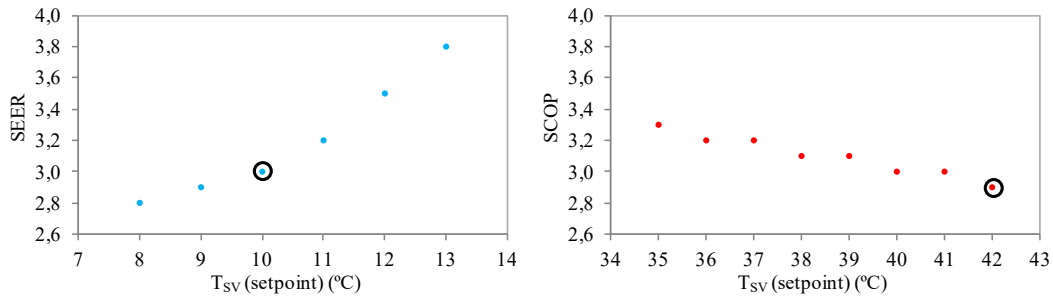


Figure 7: Simulated values of SEER (left) and SCOP (right) varying the mean inlet temperature at the evaporator (warm season) and at the condenser (cool season), respectively. The encircled dots correspond to the current values.

The next parameter explored was the electrical consumption of the circulation pumps (P_{pump}). The current input value in GLD is 1.73 kW, which corresponds to the maximum power consumption of the circulation pumps in the actual SGE installation. Values ranging from 0.7 to 2 kW were simulated and the results are shown in Figure 8. The system is especially sensitive for the warm season. Notice that $P_{pump} = 1.54$ kW if a single compressor is ON, while $P_{pump} = 1.73$ kW with both compressors ON. Given the lower values of peak load that take place during the warm season compared to the cool one (~35 kW compared to ~65 kW), the ratio between P_c and P_{pump} is lower than the ratio between P_h and P_{pump} , so a change in P_{pump} causes a more pronounced change in the simulated values of SEER. Again, these results do not mean that P_{pump} could be reduced by a 50 % or more in order to improve seasonal performance. However, it could be justified to shift to variable-speed circulation pumps which could adapt the value of P_{pump} according to the load level. The efficacy of such a measure was already demonstrated by Edwards and Finn (2015), although it requires a smart control routine.

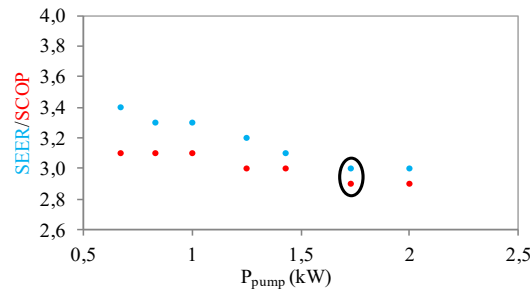


Figure 8: Simulated values of SEER and SCOP varying the power consumption of the circulation pumps. The encircled dots correspond to the current $P_{\text{pump}}=1.73$ kW

Additional simulations were run in order to assess how optimal is the actual configuration of the BHE field. In Figure 9, actual (left) and “optimised” (right) BHE field characteristics are presented. The different alternatives chosen aimed to reduce the resulting borehole thermal resistance as much as possible. The obtained value was less than 50% of the actual thermal resistance, but the simulated values of SEER and SCOP only increased from 3.0 to 3.1 and from 2.9 to 3.0, respectively. Therefore, the current borehole field should be considered quite close to optimum.

Calculated Borehole Equivalent Thermal Resistance	
Borehole Thermal Resistance: 0,152 m ² K/W	
Pipe Parameters	
U-Tube Configuration <input checked="" type="radio"/> Single <input type="radio"/> Double <input type="radio"/> Coaxial	Borehole Diameter Borehole Diameter: 130,0 mm
Backfill (Grout) Information Thermal Conductivity: 1,51 W/(m ² K)	
Check Pipe Tables	
Pipe Resistance: 0,074 m ² K/W Pipe Size: 1 1/2 in. (40 mm) Outer Diameter: 40,01 mm Inner Diameter: 32,72 mm Pipe Type: SDR11-OD Flow Type: Laminar	Radial Pipe Placement <input type="radio"/> Close Together <input checked="" type="radio"/> Average <input type="radio"/> Along Outer Wall
Calculated Borehole Equivalent Thermal Resistance	
Borehole Thermal Resistance: 0,070 m ² K/W	
Pipe Parameters	
U-Tube Configuration <input type="radio"/> Single <input checked="" type="radio"/> Double <input type="radio"/> Coaxial	Borehole Diameter Borehole Diameter: 100,0 mm
Backfill (Grout) Information Thermal Conductivity: 2,50 W/(m ² K)	
Check Pipe Tables	
Pipe Resistance: 0,041 m ² K/W Pipe Size: 3/4 in. (20 mm) Outer Diameter: 20,0 mm Inner Diameter: 16,4 mm Pipe Type: SDR11-OD Flow Type: Turbulent	Radial Pipe Placement <input type="radio"/> Close Together <input type="radio"/> Average <input checked="" type="radio"/> Along Outer Wall

Figure 9: Model settings in GLD corresponding to the borehole geometry and characteristics. The left panel corresponds to the actual SGE installation, and the right panel corresponds to a set of possible improved characteristics devoted to reduce the effective borehole thermal resistance.

Finally, it was simulated a new scenario where the load was simply doubled without considering higher peak loads and keeping the rest of the elements unchanged (same heat pump, same BHE field, etc.). The resulting SEER and SCOP were 3.0 and 2.8 respectively, almost identical to the values obtained for the current situation. This simulation would correspond to a scenario where a similar new building would be constructed adjacent to the current one. The current PLR (or load factor) at the office building is well below 0.5 [García-Céspedes et al., 2019a], so it make sense that the current BHE field and even the current GSHP machine could meet the demand in this new situation, without additional equipment and paying attention to the minimum values achieved by $T_{\text{brine}}^{\text{in}}$ (maybe a portion of Ethylene Glycol should be added to the water). However, the keypoint is to check whether the daily PLR is generally under 0.5, because then it could be feasible to divert the heat production or rejection towards both buildings alternatively via a smart control unit. Figure 10 shows how the PLR is well below 0.5 during July, but in January there are many days where the PLR is close to this value, both below and above it. This means that although in theory the current SGE installation could meet twice the current heating and cooling demands, it would be reasonable to install a support unit for the cases when both buildings could show a PLR over 0.5 simultaneously. But in any case, this support unit should be thought as a cost effective solution, not necessarily based on a renewable source.

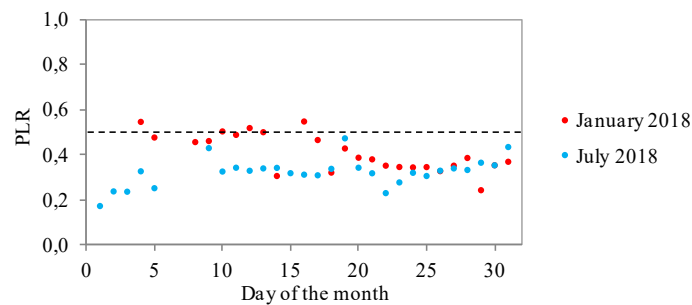


Figure 10: day-based PRL of the current SGE installation for the months with the highest heating and cooling loads.

5. CONCLUSIONS

Data-driven analysis has demonstrated to provide a large amount of useful information that cannot be extracted directly from the user interface of the monitoring system, and which can go unnoticed by classic inspection routines.

As a summary, the 3-valve problem caused an unwanted waste of heat from the DHW vessel during the warm season, which finally was absorbed by the ground. The cooling recorded as heating could be interpreted as heat demand that sooner or later would be met by the GSHP. So the amount of E_{DHW} recorded before the re-allocation of sensors T_{DHW}^{in} and T_{DHW}^{out} was an indirect (but close) measure of heat that was produced for DHW after all, indeed. The effect on the SEER was a reduction of it (although it can hardly be quantified) during the warm season. The way the 3-way valve affects to the overall SCOP is not clear during the cool season, because the leaking heating fluid would end to a “useful” place in any case. Therefore, no waste energy could be considered in this case.

Despite the fault detection, the performance degradation identification, the partialisation losses and the physical intervention from August of 2018, the WA-COP and WA-EER values still shows a decreasing trend that justifies the need of further inspection and physical interventions. From the analysis, it is concluded that the origin of this degradation in performance is neither at the side of the BHE field, nor at the building side, so the focus must be put on the production side of the SGE installation.

The results of the simulations carried out under GLD environment suggest that some minor changes could be done in the SGE installation with a resulting increase in performance. On the one hand, the current static setting of $T_{sv}^{setpoint}$ now limits the capabilities of the heat pump to operate optimally on its own. On the other hand, variable-speed circulation pumps would contribute to raise the values of SEER and SCOP. Finally, according to the simulations, the current characteristics of the BHE field are satisfactory enough from the optimisation point of view.

Interestingly, according to the simulations the SGE installation under study could meet twice the current heating and cooling loads if the peak load was kept unaltered. This is a very important result, since it tells us that, from a practical perspective, another building with similar characteristics could benefit from the current BHE field and GSHP with little investment on the production side.

ACKNOWLEDGEMENTS

This work was supported by a grant from the Institut Cartogràfic i Geològic de Catalunya (ICGC) in the framework of the general research line on shallow geothermal energy.

REFERENCES

- Edwards K. C., Finn D. P.: Generalised water flow rate control strategy for optimal part load operation of ground source heat pump systems, *Applied Energy* **150**, (2015), 50-60 <https://doi.org/10.1016/j.apenergy.2015.03.134>
- EN 14511, Air conditioners, liquid chilling packages and heat pumps with electrically driven compressors for space heating and cooling (2008)
- García-Céspedes J., Arnó G., Herms I., De Felipe J. J.: Characterisation of efficiency losses in ground source heat pump systems equipped with a double parallel stage. A case study, *Renewable Energy* (in press) (2019a) <https://doi.org/10.1016/j.renene.2019.01.029>
- García-Céspedes J., Arnó G., Herms I., De Felipe J. J.: Characterization of shallow geothermal energy installations through remote minute-resolved monitoring. A case study, *Proceedings, European Geothermal Congress, The Hague, 11-14 June* (2019b) ID44. <http://europeangeothermalcongress.eu/wp-content/uploads/2019/07/44.pdf>
- Spitler J.D. and Gehlin S., Measured Performance of a Mixed-Use Commercial-Building Ground Source Heat Pump System in Sweden, *Energies* **12**(10), (2019), 2020. <https://doi.org/10.3390/en12102020>
- Thermal dynamics Inc., Ground loop design, version 2016